A MODEL FOR VISCOELASTIC CONSOLIDATION OF WOOD-STRAND MATS. PART II: STATIC STRESS-STRAIN BEHAVIOR OF THE MAT

Elemer M. Lang

Post-Doctoral Fellow

and

Michael P. Wolcott[1]

Associate Professor

Division of Forestry
West Virginia University
Morgantown, WV 26506-6125

(Received April 1995)

ABSTRACT

A solid mechanics model is developed to predict the static stress-strain behavior of randomly formed wood-strand mats during pressing. The procedure includes a Monte Carlo simulation for reconstructing the mat structure. During the early stages of mat displacement, the model computes the cumulative stress development from strand bending. As consolidation continues, the overlapping strands form solid columns. Hooke's Law, modified by a nonlinear strain function, governs the stress development in a finite number of these imaginary columns comprising the mat. Experimental results showed good agreement with the predicted stress response.

Keywords: Wood-strand mats, consolidation, stress, compression strain, nonlinear strain function.

INTRODUCTION

Recently, several publications have dealt with a theoretical (Steiner and Dai 1994) and empirical (Lang and Wolcott 1995) description of mat structure. These works provide a rationale for the statistical description of mat structure and are based on the conceptual model of mat deformation that was developed by Suchsland (1959, 1962). Both the mat structure and the conceptual model have provided a basis for a mathematical model of mat consolidation (Dai and Steiner 1993). This model can be used to predict a number of variables important to panel consolidation including: panel void volume, densification of the wood, bonded area, horizontal density distribution, and internal stress distribution. Although this model adequately predicts the behavior of ideal flake mats, it does not account for the cumulative effect of flake bending, which dominates the lower stress region of consolidation. In addition, the description of mat structure is dependent on a theoretical description, which may not accurately represent real strand mats.

This paper presents a detailed description of a mat consolidation model that incorporates cumulative bending stresses and an empirical characterization of mat structure. Although the early stages of consolidation appear insignificant when viewing an average mat stress-strain relationship, they are crucial to the effective production of low density panels.

OBJECTIVES

The objective of this research is to develop a model, based on solid mechanics, to predict the static stress-strain behavior of simulated

[1] Present address: Wood Materials and Engineering Lab, Washington State University, Pullman, WA 99164.

Wood and Fiber Science, 28(3), 1996, pp. 369–379

wood-strand mats. A Monte Carlo simulation has already been developed to describe the spatial structure of such mats (Lang and Wolcott 1995). The specific objectives of the research presented here are:

1. Develop a mathematical model based on solid mechanics to approximate the stress response of randomly formed strand mats in compression.
2. Experimentally validate the model by comparing the behavior of realistic mats to the model predictions.
3. Determine the sensitivity of the model prediction to changes in variables describing the mat structure.

THEORETICAL BACKGROUND AND MODEL DEVELOPMENT

During manufacture of nonveneer wood-based composites, a loosely formed mat is compressed to a target thickness. This pressing reduces the voids within the mat and provides contact between adjacent particles to promote adhesion. The compression force applied to the mat can be plotted against time as shown in Fig. 1a. This curve can be divided into three different regions: (1) press closing, (2) stress relaxation, and (3) venting (Wolcott et al. 1990). During press closing, stress develops nonlinearly with displacement from the structural and material nonlinearity of the mat. This region can be converted into a stress-strain diagram as shown on Fig. 1b. Note that the stress is plotted in logarithmic scale to magnify the lower stress region. By examining this diagram, the following observations can be made:

1. The stress development is minimal at the beginning of the consolidation.
2. As the displacement continues, the stress increase becomes continuous and smooth as the individual strands deform in bending.
3. Rapid stress development can be observed for mat strains greater than 60%, where consolidation is dominated by the compression of solid wood strands.

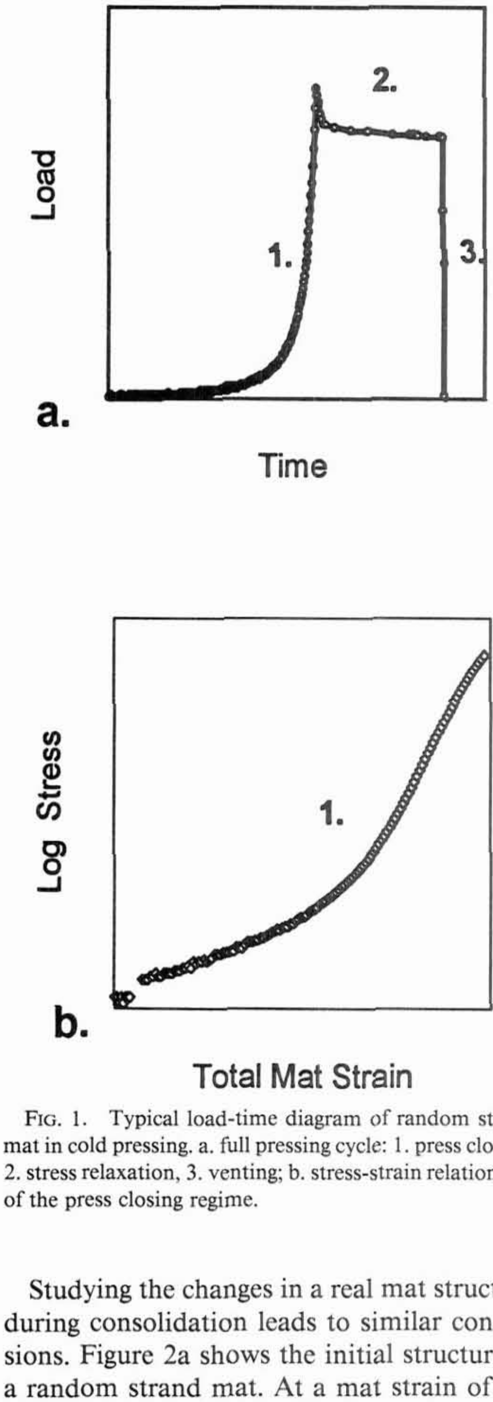

FIG. 1. Typical load-time diagram of random strand mat in cold pressing. a. full pressing cycle: 1. press closing, 2. stress relaxation, 3. venting; b. stress-strain relationship of the press closing regime.

Studying the changes in a real mat structure during consolidation leads to similar conclusions. Figure 2a shows the initial structure of a random strand mat. At a mat strain of approximately 30%, the void heights decrease and the curved strands flatten (Fig. 2b). When the total mat strain is approximately 60%, the void heights approach a minimum value (Fig. 2c).

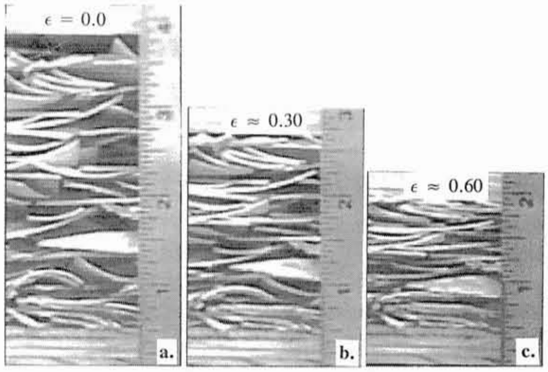

FIG. 2. Structural changes in a random strand mat during consolidation. a. initial bulk structure; b. at total mat strain $\epsilon \approx 0.3$; c. at strain $\epsilon \approx 0.6$.

Based on the previous observations and results of earlier research projects (Suchsland 1962; Harless et al. 1987; Suchsland and Xu 1989; Dai and Steiner 1993, 1994a, b), it is assumed that the static compression response of a strand mat can be separated into two components. In the early stage of the consolidation, the cumulative stress development results from the bending resistance of the individual strands. As consolidation continues, overlapping strands form solid columns of varying height that deform in transverse compression.

To facilitate numerical solution for the stress development, a 19- × 19-mm base column was chosen as the smallest theoretical unit of the mat (Fig. 3a). Each column is characterized by the number of overlapping strands (N_{bj}) and the void heights (Δ_{bjk}) between consecutive strands. In addition, the connectivity between adjacent columns is determined by quantifying the distance of the column centroid to the strand end (X_{bjk}). A mat is divided into experimental units (152 × 152 mm) termed as a mat block. Each block contains 64 columns, 32 at the edges, from which the stochastic parameters of the mat structure were obtained for simulation (Lang and Wolcott 1995). Thus, subscripts b, j, k are the experimental block, column and strand indexes, respectively. The following theories were used to predict the stress response of a column to compression strain.

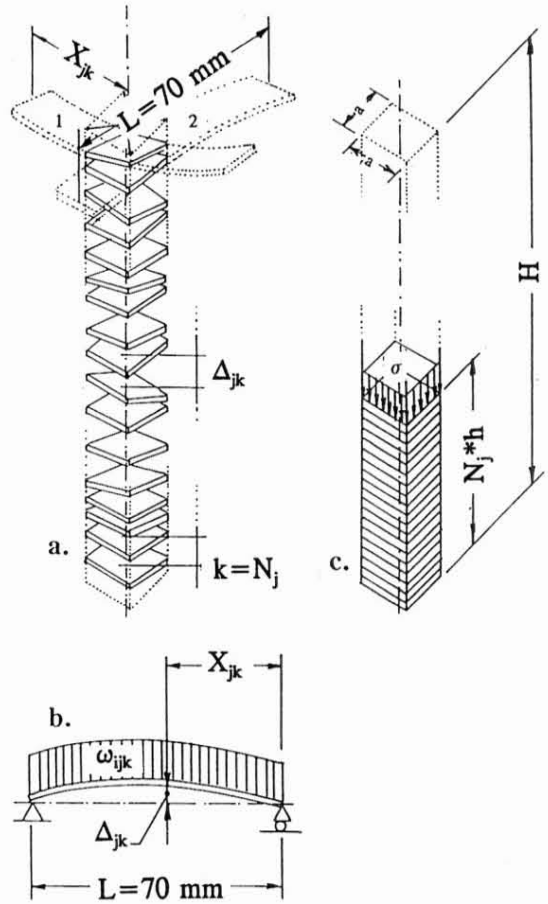

FIG. 3. The theoretical unit of the static stress-strain model. a. idealized initial structure of a column; b. the 'beam' model; c. the solid strand stacking.

Stresses due to strand bending

To maintain the simplicity and mathematical tractability of the model, several assumptions were made. Each strand was considered as a small, simply supported beam under distributed load (Fig. 3b). The beam deflection was determined at the column centroid, and the location variable (X_{bjk}) identified the position of an individual strand relative to the column centroid. The maximum deflection of the strand beam was defined by the adjacent void height. An inverted form of a beam deflection equation was used to determine the distributed load necessary to deflect the strand beam and form a solid strand column.

The limitation of this idealized strand bending model is that in reality, several strands in each column support point loads at the beginning of the consolidation. Furthermore, as consolidation proceeds, the spacing and number of supports for a strand beam will change. These phenomena were modeled by proportionally decreasing the beam (strand) span and modifying the location variable with the applied displacement.

To quantify the stress development in a column, the total mat displacement is proportionally assigned to each strand. The necessary distributed load to cause this deflection is then calculated as follows:

$$\omega_{ijk} = \frac{\Delta_{ijk} X_{ijk} 24EI}{L_{ijk}^3 - 2L_{ijk}^2 + X_{ijk}^3} \quad (1)$$

where:

- ω_{ijk} = distributed load (N/m)
- Δ_{ijk} = proportional deflection of the strand (m)
- X_{ijk} = location of the column centroid (m)
- E = MOE in bending of the strand (Pa)
- I = moment of inertia (m^4)
- L_{ijk} = changing length of the beam (m)
- $_i$ = index of the total mat strain (ϵ)
- $_{jk}$ = column and strand index, respectively

The obtained distributed load values can be converted into stress by the following summation:

$$\sigma_{ij} = \sum_{k=1}^{N_j} \frac{\omega_{ijk}}{a} \quad (2)$$

where:

- σ_{ij} = stress in column j at strain i (Pa)
- N_j = number of overlapping strands in column j
- a = width of the column (strand) (m)

The total mat displacement is distributed proportionally to the strands until the total void height is eliminated or the target thickness has been achieved. Since each strand has a different maximum deflection value (i.e., different void heights between the strands), the stress computation stops when the proportional displacement is equal to the void height (Δ_{jk}) associated with the strand. Then, this particular strand is assumed to be perfectly flat and in a horizontal position. The corresponding stress value is preserved, and the proportional displacements are increased for the remaining strands. The procedure continues until all void spaces are eliminated and the column is compressed to a solid, layered strand block (Fig. 3c). Note, while using this approach to describe the stress-strain relationship during the early stage of consolidation, the strand orientation has no explicit influence on the stress development.

Stress development in solid strand columns

When the voids in a column have been eliminated by mat compression, the strands have developed bending but not compression stresses. As consolidation continues toward the target mat thickness, columns begin to undergo compression strain.

The compression behavior of wood strands can be modeled using theories of cellular materials. The characteristic stress-strain curve of wood in transverse compression has been discussed in detail by several authors (Maiti et al. 1984; Wolcott et al. 1989b; Wolcott 1990; Dai and Steiner 1993). Hooke's Law modified with a nonlinear strain function ($\Phi(\epsilon)$) can be used for a constitutive relation (Rush 1969; Wolcott et al. 1989a):

$$\sigma = E\epsilon\Phi(\epsilon) \quad (3)$$

where:

- σ = compressive stress
- ϵ = strain
- E = Young's modulus of the cellular material
- $\Phi(\epsilon)$ = nonlinear strain function

The nonlinear strain function can be determined experimentally by compressing strand columns. The linear regime of the corresponding stress-strain relationship is analyzed to determine the Young's modulus. The values of the nonlinear strain function can then be calculated by rearranging Eq. (3) and described using an empirical polynomial (Dai and Steiner 1993).

In the absence of experimental data, structural theories developed for honeycomb and closed cell foams may be applied to determine $\Phi(\epsilon)$ with the resulting equation (Wolcott et al. 1989b):

$$\Phi(\epsilon) = \frac{C_3/C_2}{\epsilon}\left[\frac{1 - \rho_r^{1/3}}{1 - \rho_r(\epsilon)^{1/3}}\right]^3 \quad (4)$$

where:

ϵ = compressive strain
ρ_r = relative density of the wood
$\rho_r(\epsilon)$ = changes of relative density
C_3 = yield strain (ϵ_y)
C_2 = linear elastic constant
$\Phi(\epsilon)$ = nonlinear strain function in transverse compression

In this equation the relative density is defined as the ratio between the solid wood density and the cell-wall density. The linear elastic constant is a function of the strand thickness. The changes of relative density ($\rho_r(\epsilon)$) can be computed from the relationship between the plastic strain and the expansion ratio as follows:

$$\rho_r(\epsilon) = \rho_r[1 - \epsilon_p + \tfrac{2}{3}\mu\epsilon_p - \mu\epsilon_p^2]^{-1} \quad (5)$$

where:

ϵ_p = plastic strain = $\epsilon - \epsilon_y$
μ = expansion ratio

The expansion ratio is defined as the ratio of lateral strain to compressive strain in the nonlinear stress-strain region (Wolcott et al. 1989a).

In both approaches, the value of $\Phi(\epsilon)$ is equal to unity for strains less than ϵ_y. Equation 4 becomes singular as the relative density (ρ_r) approaches 1 (i.e., total densification of the cellular material). However, total densification seldom occurs during manufacture of wood-based composites.

Mat behavior

The constitutive relationships have been defined to predict the stress response of strand columns in compression. This model must now be extended to include the stochastic nature of spatial characteristics within the mat as input values for the computations. To achieve this, Dai and Steiner (1993) based their prediction on Eq. (3) combined with the formula for the Poisson(λ) probability distribution to obtain the nominal stress development through an infinite summation. The model presented here combines the bending resistance of strands early in consolidation with an empirically derived mat structure. The spatial mat structure is defined by three variables: overlapping strand numbers (N_{bj}), void heights (Δ_{bjk}), and strand location (X_{bjk}). For computational purposes, a multiple-step simulation is used to generate these variables from normal, lognormal, and Poisson probability distributions (Lang and Wolcott 1995). The nominal stress response is then computed as the average stress development in the strand columns.

One advantage to this approach is that consolidation can be predicted from the individual experimental units (sample blocks) by using actual measured parameters as inputs. These predictions can then be compared to the experimental results for validation.

Different computational steps are required for simulation and stress prediction. In the initial stage of the model (steps 1–3), the mat structure is reconstructed on a probabilistic basis as reported by Lang and Wolcott (1995). Steps 4–8 are the stress calculations for a mat section (block). Step 9 improves the resolution and usually n = 5 was found to be adequate. The following list summarizes the model structure:

1. Generate the mean overlapping strand numbers (λ_b) in a mat block: $\lambda_b \in N(\mu, \sigma^2)$.
2. Generate the number of overlapping strands (N_{bj}) for the 64 columns in block b: $N_{bj} \in$ Poisson(λ_b).
3. Generate and assign location (X_{bjk}) and void

height (Δ_{bjk}) data for each strand in each column: $X_{bjk} \in \ln(\mu, \sigma^2)$ and $\Delta_{bjk} \in \ln(\mu, \sigma^2)$.

The stress is then calculated for a mat as follows:

4. Assign an incremental total mat displacement.
5. Compute the proportional deflection of each strand in a column. Calculate the cumulative stress in the column according to Eqs. (1) and (2).
6. If $\Sigma\,\Delta_{bjk} \leq$ the total mat displacement, compute the stress by Eq. (3).
7. Repeat steps 5 and 6 for the 64 columns. Calculate the average stress. Print total mat strain (ϵ) and stress (σ).
8. Repeat steps 4–7 until the target mat thickness is reached.
9. Repeat steps 1–8 for each of n blocks comprising a mat and calculate the average stress response.

The stress prediction requires inputs for the Young's modulus of strands in bending and transverse compression. The bending modulus $E_b = 1.58 \times 10^6$ (psi) value was obtained from the literature (USDA Forest Service 1982). The compression modulus E_c was determined experimentally.

EXPERIMENTAL VALIDATION OF THE MODEL

Materials

Yellow-poplar (*Liriodendron tulipifera*) strands (0.8 × 19 × 70 mm) were manufactured using a laboratory flaker. The faces of the strands were random cuts between the radial and tangential directions. After manufacture, the strands were oven-dried and preconditioned at 25°C and 65% relative humidity assuring 11 ± 1% moisture content.

The sample mats (blocks) were hand-formed in a 305- × 305-mm box using 702-g strands. The 76.5-mm-wide mat edges, where the strand alignment might be influenced by the forming box, were removed with a large paper shear. The final dimensions of the experimental mat blocks were 152 × 152 mm at base and ca. 75 mm in height (Lang and Wolcott 1995), with an average bulk density of 100 kg/m³. The average target density was 600 kg/m³ when pressed to a 13-mm final thickness.

For determining the compression modulus, twelve 19-mm-square strands were stacked to form a solid column. Nine strand columns were conditioned and prepared for compression testing.

Methods

Compression tests for both mat blocks and solid strand columns were conducted on a universal servo-hydraulic testing machine equipped with a 90-kN load cell. The machine compliance was determined prior to testing, and the test results were corrected accordingly. The loading rate for both tests was 6 mm/min. A computerized data acquisition system collected the load and displacement data in real time.

RESULTS AND DISCUSSION

Material property tests

From the nine solid strand columns tested in compression, the mean of E_c was estimated to be 4.2 MPa, while the mean yield strain (ϵ_y) was found to be 0.14. These values are comparable to those reported by Wolcott et al. (1989a) with yellow-poplar strands.

An empirical strain function ($\Phi(\epsilon)$) was approximated by fitting a tenth-order polynomial to the data above the yield strain. Table 1 contains the approximated regression coef-

TABLE 1. *The approximated regression coefficients for the empirical strain function ($\Phi(\epsilon)$).*

Coefficient	Value
β_0	0.71
β_1	5.19
β_2	−53.13
β_3	295.24
β_4	−1,114.44
β_5	2,917.08
β_6	−5,269.65
β_7	6,578.05
β_8	−5,307.15
β_9	2,459.07
β_{10}	−528.69

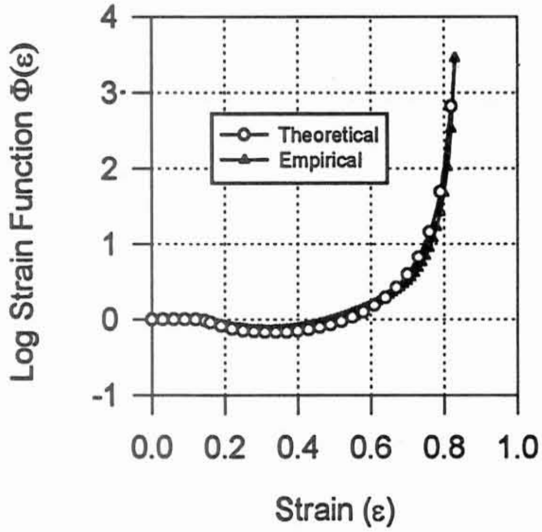

FIG. 4. Comparison of the strain functions obtained by polynomial fitting and by theory (Eq. 4).

ficients. The theoretical strain function defined by Eq. (4) is graphically compared to the empirical result in Fig. 4. Good agreement can be observed between the two strain functions.

Experimental and model predicted behavior of mat blocks

For validation, the average overlapping strand numbers (λ_b) were experimentally determined for five sample blocks and used as input for simulating the mat structure. This parameter provided a link between the experimental and predicted data for each block. During this procedure, the average stress-strain behavior of 64 strand columns was modeled. The five experimental and predicted stress-strain relationships are compared in Fig. 5. In general, good agreement was found. For the mat blocks used, approximately 60–65% compression was required to initiate a rapid stress development. The model tends to overpredict stress in the densification region, although this error does not appear to be major.

Mat stress-strain behavior

To simulate a larger mat, another five sample blocks were prepared and tested. The mean overlapping flake number from 160 columns along the perimeters of the five sample blocks was used to generate λ_b values for each block (step 1). Figure 6a shows the comparison of the average predicted and the experimental stress-strain behavior of the five mat blocks. A significant improvement is observed in the prediction quality of the model as compared to the individual blocks. In this case the model prediction is based on the average stress response of 320 theoretical units (columns). Although the model still slightly overpredicts the stress response, this error is not as severe as in the individual blocks, and the slope of the predicted and experimental curves shows good agreement. Improving the resolution (i.e., simulating more than five sample blocks) did not result in a better approximation of the stress response, but the computation time increased significantly.

Low stress consolidation

To amplify the response of the low stress region, the average experimental and predicted responses are shown in logarithmic scale (Fig. 6b). While no significant deviation could be observed on the normal scale, below 0.01 MPa the cumulative strand bending does not properly predict the stress response. Dai and Steiner (1993) reported accurate prediction down to 1.5 MPa of mat stress. Their model was adapted to the yellow-poplar mat used in this research (Fig. 6). By including the contribution of strand bending to dissipate voids, the model presented here predicts accurately to stress of 0.1 MPa. This strand bending model approximates the stress-level when the individual strands are connected in each column; however, it does not predict the entire process. Although both approaches predict the mechanical behavior of mats in high stress regions, an understanding of the low stress consolidation is not yet complete. Further research is needed to explore the consolidation mechanism in the low stress region, which is extremely important when pressing low-density materials.

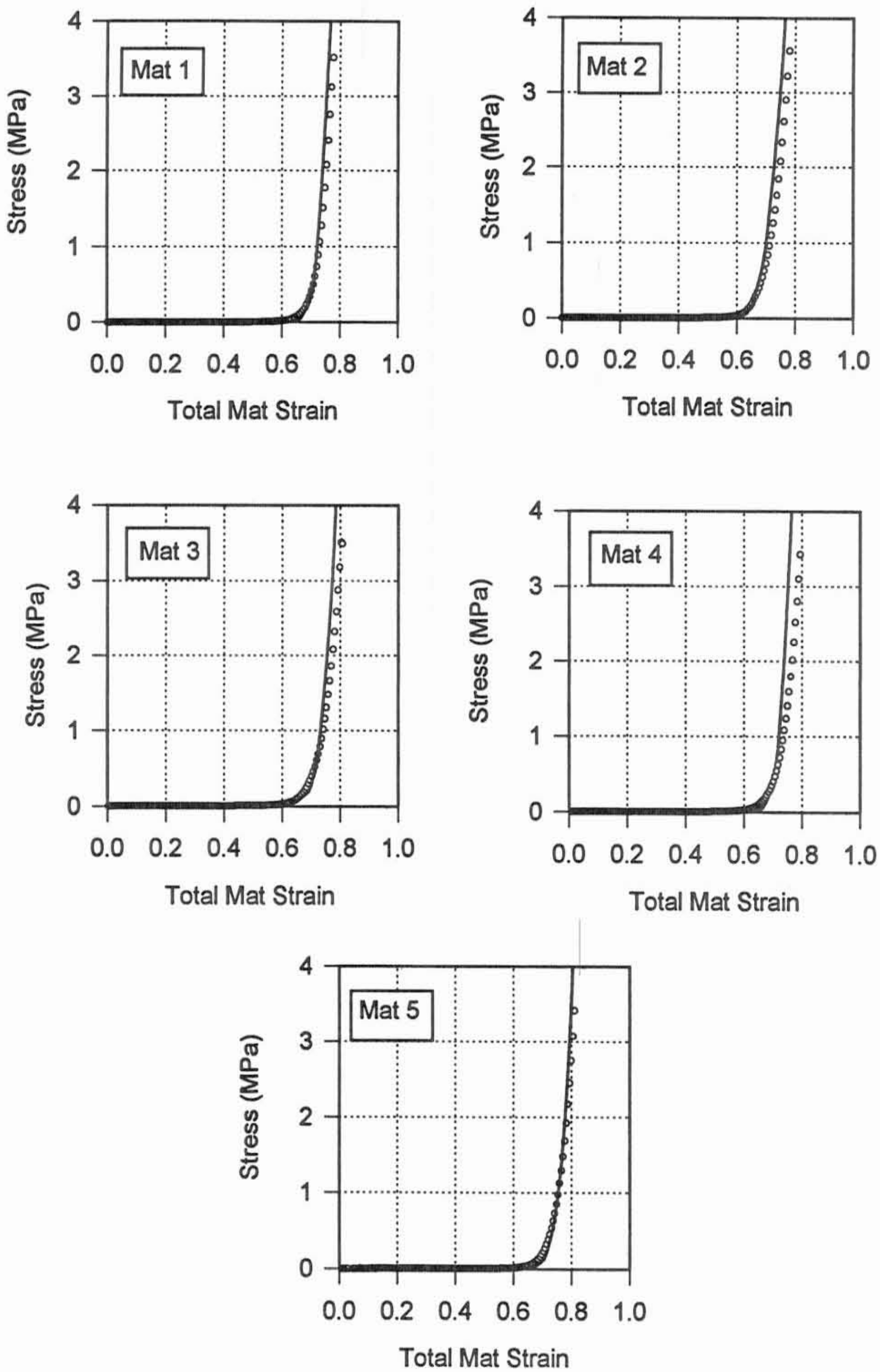

FIG. 5. Results of the model validation. The stress prediction was based on 64 columns simulation in a mat block using the average overlapping strand numbers (λ_b) obtained from measurements of the actual mats. Symbols and lines represent the experimental and predicted data, respectively.

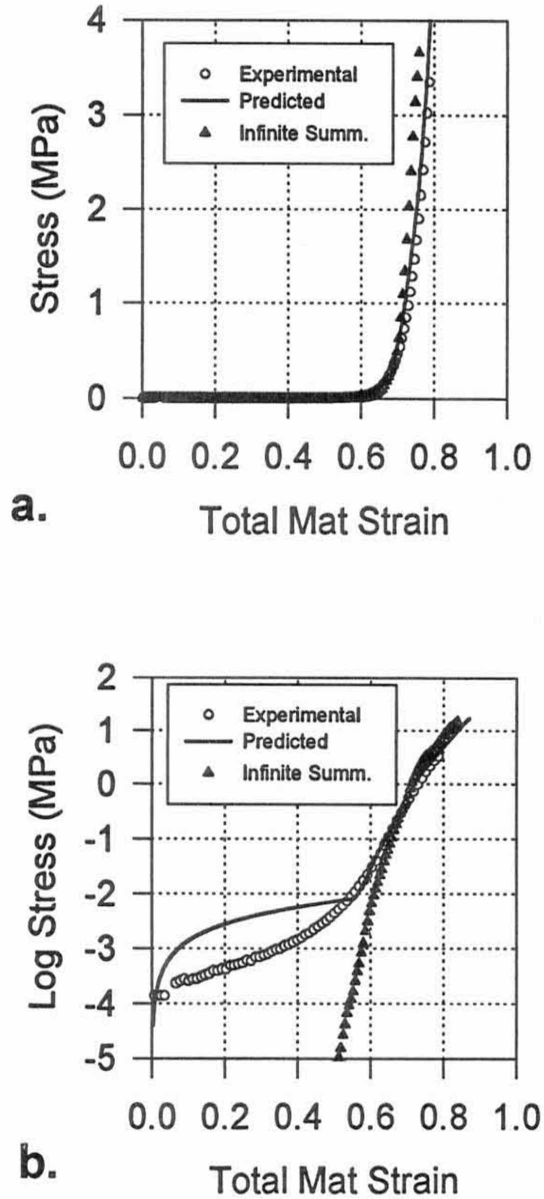

FIG. 6. Final result of the model validation. The average experimental stress response of five sample mats compared to the model prediction. a. linear scale; b. logarithmic scale.

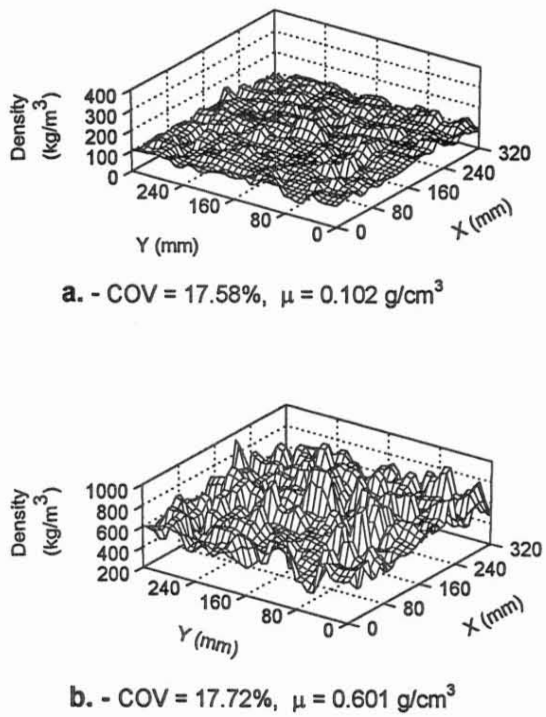

FIG. 7. Horizontal density distribution of five sample blocks (324 × 324 mm mat area). The coefficients of variation and mean values are listed. a. mat bulk density; b. panel target density at 13 mm target thickness.

Other mat characteristics

Predicting consolidation is not limited to the overall mat stress-strain relationship. The five sample blocks used for model validation depict a 324- × 324-mm mat area. Using the simulated N_{bj} ($b = 1, \ldots, 5$ and $j = 1, \ldots, 64$) data, the bulk (i.e., mat) and target densities of the 320 columns were computed (Fig. 7). From simulation, the average bulk density of the mat and the target density for the panel are 102 and 601 kg/m³, respectively. These values show excellent agreement with the observed densities of 100 and 600 kg/m³, indicating that the simulation procedure accurately reconstitutes the mat structure and preserves the density characteristics. The coefficient of variation for the in-plane density is slightly higher for the panel (17.72%) than the bulk (17.58%) because some of the columns undergo densification during pressing.

The residual void volume may be calculated through the simulation by determining the columns that do not fully consolidate. In 19 of the 320 columns, the sum of the strand thicknesses is less than the panel target thickness.

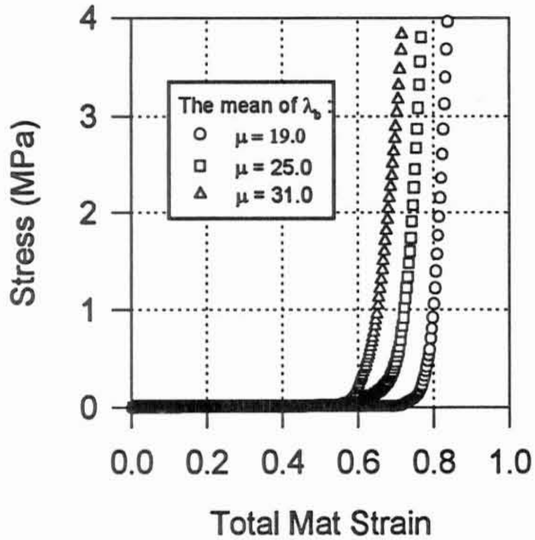

FIG. 8. Model sensitivity to the mean overlapping strand number (λ_b) in an experimental block (64 columns).

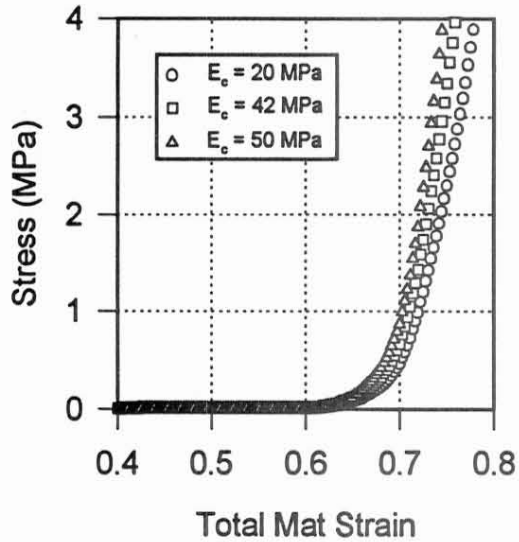

FIG. 9. Model sensitivity to the compression modulus of solid strand columns.

These nineteen columns represent 6% of the total mat area where the adhesion might be inadequate.

Sensitivity studies

The purpose of the sensitivity analysis was to determine if the variability of a particular input property has a significant effect on the model prediction. When holding all other variables constant, the variability in the mean overlapping strand number (λ_b) has the strongest effect on the stress prediction by controlling the mat strain when strand compression begins (Fig. 8). In turn, the E_c for the wood strand influences the slope of the rapid stress development. In Fig. 9, the 25 MPa compression modulus represents aspen strands as reported by Dai and Steiner (1993); 42 MPa was experimentally determined for yellow-poplar during this study and the 50 MPa may depict the behavior of high density strands (i.e., SG > 0.5). The increasing standard deviation of the location (X_{bjk}) variable slightly increased the stress development during strand bending. The increasing variability of void height (Δ_{bjk}) resulted in decreasing stress development. No significant effect of these variables could be detected on the stress development in the higher stress region. However, it should be noted that the shape, length, width, and orientation of the strand may be strongly correlated to these variables and might influence significantly the low stress consolidation.

SUMMARY AND CONCLUSIONS

A mathematical model for predicting the static stress-strain response of randomly formed strand mats is presented. In this model the mat structure is considered as a finite number of imaginary columns, varying numbers of overlapping strands and size of void space. The stress approximation is based on simple beam theory and the compression behavior of cellular materials. The non-linearity resulting from the macro-structure of the mat is considered and modeled on a stochastic basis.

The described model can predict the stress response of randomly formed mats with good accuracy over 0.01 MPa. The experimental results and the analytical work resulted in the following conclusions:

1. The compression modulus (E_c) of the strands and the nonlinear strain function ($\Phi(\epsilon)$) de-

termine the slope of the mat stress-strain curve in the cellular collapse and densification region.
2. The mean value of the overlapping strand numbers in a mat governs the strain when strands begin to deform in compression.
3. The in-plane variability of the overlapping strand numbers governs the horizontal density distribution, residual void volume, and unbounded area in the panel.
4. Because the strand deposition mainly depends on the mat formation technique, the panel structure may be improved by modifying the mat forming process.

This model was validated with random strand mats constituted from uniformly sized, yellow-poplar strands. The simulation routines are based on empirical probability distributions and do not generally apply to all mat structures. However, theories for the structural simulation and consolidation process have universal value. The model is easily adaptable to realistic mat structures. Since the model is comparatively simple, it provides a good basis for further improvement which includes the time, temperature, and moisture interaction during hot pressing and stress relaxation under constant mat strain.

ACKNOWLEDGMENTS

The financial support through the USDA National Research Initiative Competitive Grants Program, Agreement No. 91-37103-6642, is gratefully acknowledged. The authors wish to express their appreciation to Dr. Frederick Kamke and Christopher Lenth for their contribution to this research at the Department of Wood Science and Forest Products, Virginia Polytechnic Institute and State University. This manuscript is published as Scientific Article no. 2517 of the West Virginia Agriculture and Forestry Experiment Station.

REFERENCES

Dai, C., and P. R. Steiner. 1993. Compression behavior of randomly formed wood strand mats. Wood Fiber Sci. 25(4):349–358.

———, and ———. 1994a. Spatial structure of wood composites in relation to processing and performance characteristics. Part 2. Modelling and simulation of a randomly-formed strand layer network. Wood Sci Technol. 28(2):135–146.

———, and ———. 1994b. Spatial structure of wood composites in relation to processing and performance characteristics. Part 3. Modelling the formation of multi-layered random strand mat. Wood Sci. Technol. 28(3): 229–239.

Harless, T. E. G., F. G. Wagner, P. H. Short, R. D. Seale, P. H. Mitchell, and D. S. Ladd. 1987. A model to predict the density profile of particleboard. Wood Fiber Sci. 19(1):81–92.

Lang, E. M., and M. P. Wolcott. 1996. A model for viscoelastic consolidation of wood-strand mats. Part I: Structural characterization of the mat via Monte Carlo simulation. Wood Fiber Sci. 28(1):100–109.

Maiti, S. K., L. J. Gibson, and M.F. Ashby. 1984. Deformation and energy absorption diagrams for cellular solids. Acta Metall. 32(11):1963–1975.

Rush, K. C. 1969. Load-compression behavior of flexible foams. J. Appl. Polym. Sci. 13:2297–2311.

Steiner, P. R., and C. Dai. 1994. Spatial structure of wood composites in relation to processing and performance characteristics. Part 1. Rationale for model development. Wood Sci. Technol. 28(1):45–51.

Suchsland, O. 1959. An analysis of the particleboard process. Michigan Quart. Bull. 42(2):350–372.

———. 1962. The density distributions in strand boards. Michigan Quart. Bull. 45(1):104–121.

———, and Hong Xu. 1989. A simulation of the horizontal density distribution in a strandboard. Forest Prod. J. 39(5):29–33.

USDA Forest Service. 1987. Wood handbook. USDA Agric. Handb. 72 (rev.) USDA Forest Service, Forest Prod. Lab., Madison, WI. 466 pp.

Wolcott, M. P. 1990. Modeling viscoelastic cellular materials for the pressing of wood composite. Ph.D. dissertation, Virginia Polytechnic Institute and State University, Blacksburg, VA. 170 pp.

———, F. A. Kamke, and D. A. Dillard. 1990. Fundamentals of strandboard manufacture: Viscoelastic behavior of the wood component. Wood Fiber Sci. 22(4): 345–361.

———, B. Kasal, F. A. Kamke, and D. A. Dillard. 1989a. Modeling wood as a polymeric foam: An application to wood-based composite manufacture. Proc. Third joint ASCE-ASME Mechanics Conference. University of California, San Diego, LaJolla, CA. Pp. 53–60.

———, ———, ———, and ———. 1989b. Testing small wood specimens in transverse compression. Wood Fiber Sci 21(3):320–329.